Membrane Water Treatment, *Vol. 7, No. 2 (2016) 115-126*
DOI: http://dx.doi.org/10.12989/mwt.2016.7.2.115

Analysis of newly designed CDI cells by CFD and its performance comparison

Se Hwan Kwon and Ji Won Rhim*

Department of Advanced Materials and Chemical Engineering, Hannam University, 1646 Yuseongdae-ro, Yuseong-gu, Daejeon 34054 Korea

(*Received October 28, 2015, Revised January 06, 2016, Accepted January 13, 2016*)

Abstract. In this study, computational fluid dynamics (CFD) analysis was conducted to investigate the flow pattern and to find the occurrence of dead zones in an existing capacitive deionization (CDI) cell. Newly designed cells—specifically designed to avoid dead zones—were analyzed by CFD in accordance with the flow rates of 15, 25 and 35 ml/min. Next, the separation performances between the existing and newly designed cell were compared by conducting CDI experiments in terms of salt removal efficiency at the same flow rates. Then, the computational and experimental results were compared to each other. The salt removal efficiencies of the hexagon flow channel 1 (HFC1) and hexagon flow channel 2 (HFC2) were increased 88-124% at 15 ml/min and 49-50% at 25 ml/min, respectively. There was no difference between the existing cell and the foursquare flow cell (FFC) at 35 ml/min.

Keywords: capacitive deionization (CDI); dead zone; flow channel; computational fluid dynamics (CFD); cell design

1. Introduction

For the production of ultra-pure water by the utilization of ion exchange membranes, there are several processes such as the electrodeionization (EDI) process (Khoiruddin *et al*. 2014, Turek *et al*. 2013), capacitive deionization (CDI), and membrane capacitive deionization (MCDI) (Biesheuvel and van der Wal 2010), etc. EDI process is a separation process which combines of electrodialysis and ion exchange whereas CDI, first introduced by Caudle *et al*. (1966), is an electrically induced alternative approach for extracting salt ions from concentrated saline solutions. In this paper, CDI which takes an attention in recent years will be discussed in more detail.

The CDI process takes advantage of the excess ions adsorbed in the electrical double layer region at an electrode-solution interface when the electrode is electrically charged by an external power supply (Li and Zou 2011). In a CDI operation, when an electrical potential is applied to an electrode, charged ions in feed water are adsorbed onto the surface of the charged electrodes so

*Corresponding author, Professor, E-mail: jwrhim@gmail.com

 ISSN: 2005-8624 (Print), 2092-7037 (Online)

that an electrical double layer is formed at an electrode-solution interface (Park 2008). As a result, purified water is produced. In the case of a zero or reverse electrical potential, the adsorbed ions are desorbed back into the bulk feed solution and the saturated electrodes undergo regeneration; therefore, in a CDI operation, electrode performance is the key parameter for accomplishing complete adsorption and desorption within a desired period (Lee *et al*. 2011, Pei *et al*. 2008, Faisal *et al*. 2014). Also, the membrane module structure has an important role to perform an effective separation. In particular, the plate-and-frame type module needs uniform flow in both laminar and turbulent situations to avoid a dead zone where no separation occurs.

During the CDI process, cell operation as well as electrode material characteristics and membrane-bound structure can lead to a dead zone. These dead zones can be a factor affecting salt removal efficiency. Depending on the module structure, the contact states of fluid and membranes vary and affect separation performance.

Computational fluid dynamics (CFD) is used to analyze movement of a fluid which passes through or around an object. This software can predict product performance before production, optimize design, and examine effectiveness of operation. Turbulent flow models, such as DES (detached eddy simulations), LES (large eddy simulations), k-ε model and k-ω model, have been used for accurate flow analysis to simulate turbulent flow which cannot be calculated by computational fluid dynamics. Using CFD, different strategies for module design and consequently reduction of polarizations' effect would be possible prior to conducting costly experiments (Shirazi *et al*. 2016).

During the past two decades, CFD has been widely used to model the hydrodynamic behavior of membrane-separation processes using membrane modules (Schwinge *et al*. 2004, Ghidossi *et al*. 2006). The appropriate cell types in spiral-wound membrane modules have been suggested based on the three-dimensional CFD analysis of spacer-filled membrane module designs with various spacer arrangements. Li and Tung (2008a and b) noted that although the outward appearance was similar to that of a spiral channel, their results showed that the curvature of a spacer-filled channel affected the flow field in spiral-wound membrane modules.

Lin *et al*. (2006) performed laboratory-scale and pilot-scale flow analysis for a mixed solution with methanol and C_5 in the pervaporation process to analyze the process efficiency and also used the CFD flow analysis to investigate dead zones in the module. Furthermore, flow channel flux in a cell or a module through CFD flow analysis to increase efficiency has been investigated (Fontalvo *et al*. 2006). Takaba and Nakao (2005) conducted CFD flow analysis in gas separation to investigate concentration polarization and designed a membrane module in the ideal selectivity conditions for polarization. Rahimi *et al*. (2005) preliminarily analyzed membrane permeability depending on pressure by using CFD and then obtained similar results under the same conditions in the final study.

In this study, CFD analysis was conducted to investigate the flow pattern and to find the occurrence of dead zones in the existing CDI cell. On the basis of the CFD analysis, new CDI cells—designed to avoid dead zones in which the separation performance is affected—were designed. Also, this new cell was analyzed by CFD. Next, the separation performances between the old and newly designed cell were compared by conducting CDI experiments in terms of the salt removal efficiency. Finally, CFD analysis and separation performance, i.e., calculation and experimental results were mutually compared. For the flow pattern, the flow rates of 15, 25, and 35 ml/min were used in both CFD and CDI experiments. The adsorption/desorption electric potential was 1 V/0 V and adsorption/desorption time was 3 min/1 min.

2. Experimental procedures

2.1 Materials

Sodium chloride (NaCl, 99.5%) was purchased from OCI, Korea. The carbon electrode was provided by Pureechem (Chungbuk, Korea). All CDI cells were made from poly(methyl methacrylate) plates.

2.2 Simulation tool

The software used in the study was ANSYS CFX version 15.07 and the *k*-epsilon (*k*-ε) turbulent flow model was adopted. In addition, mesh was set on the basis of one million elements and it was checked that skewness was less than 0.9 for calculation. A wall condition (noninvasive condition) was established on the wall of an internal flow field because a boundary layer arises from viscosity, but not in fully developed flow. The target was an error tolerance of 0.00001. The inlet was dependent on flux setting and the outlet was set at atmospheric pressure. From the simulation, the pressure applied on a cell at each flow rate, fluid behavior at each point inside a cell, and the presence/range of a dead zone in each flow channel were analyzed.

2.3 Cell configuration

As shown in Fig. 1, the foursquare flow channel (FFC), hexagonal flow channel 1 (HFC1), and hexagonal flow channel 2 (HFC2), which angle in below part was larger than that of HFC1, were prepared for CFD analysis. The outer size of the cell was 16 cm x 16 cm and the flow channel areas of each cell were 144, 114, and 107 cm^2, respectively, for FFC, HFC1, and HFC2. The electrode area in a flow channel which was separated 1 cm from each face of the flow channel was 100, 75 and 70 cm^2 (directly measured from Fig. 1) in order, respectively again, for FFC, HFC1, and HFC2.

2.4 CDI experiment (*Lee et al. 2010*)

Schematic diagram of the CDI cell and CDI experimental apparatus are illustrated in Fig. 2.

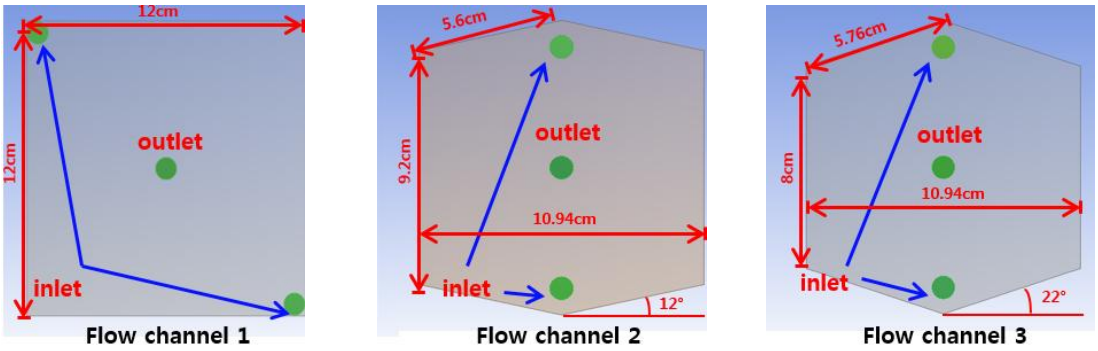

(a) Foursquare (FFC) (b) Hexagon 1 (HFC1) (c) Hexagon 2 (HFC2)

Fig. 1 Detailed size and shape of (a) the existing cell (FFC); and (b) newly designed HFC1; and (c) HFC2

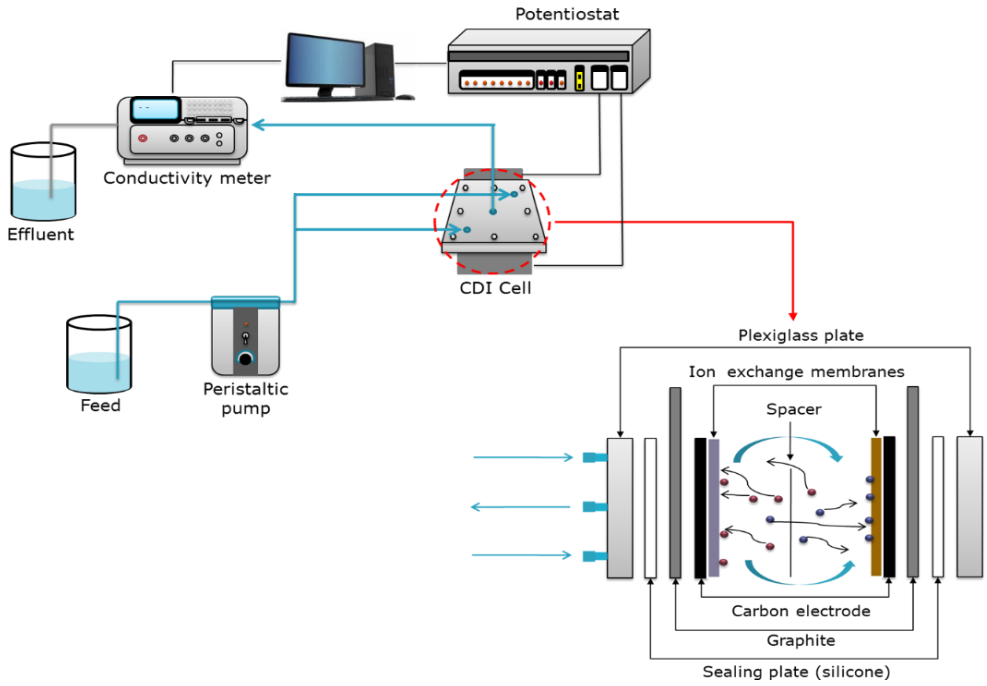

Fig. 2 Schematic diagram of experimental apparatus

The CDI system consists of a feed tank, a peristaltic pump (IWAKI, PST-100), a TDS conductivity meter (OAKATRON, Japan), a potentiostat (WPG 100, WonATech Corp.), and a CDI unit cell. This CDI unit—regardless of the shape (foursquare or hexagon)—is made of two carbon electrode sheets separated by a non-conductive spacer that prevents an electrical short and allows the feed solution to flow. Graphite sheets on both outer sides of the electrodes play the role of current collector. Two silicon sheets of 1 mm thickness lie in between the outer sides of the current collectors and the 10 mm thick Plexiglas® plate to act as seals.

A feed solution of 100~110 mg/L sodium chloride with a flow rate of 15, 25 and 35 ml/min was allowed to flow continuously into the two entry holes on the CDI unit cell surface. Water came out of the exit hole on the center of the CDI cell surface. The ion conductivity of the effluent water was measured every 3 s and recorded in the computer. Fixed potentials of 1.0 V for adsorption and 0 V for desorption were applied to the CDI cell for the adsorption/desorption time of 3 min/1 min and controlled by a potentiostat.

3. Results and discussion

3.1 CFD analysis

3.1.1 Internal pressure depending on the feed flow rate

The internal pressure was investigated for 3 types of CDI cells according to the feed flow rates (Fig. 3). In general, the internal pressure increases as the feed flow rate increases. And, the internal pressure of the FFC cell is the lowest among the cells in question. This is due to the flow channel

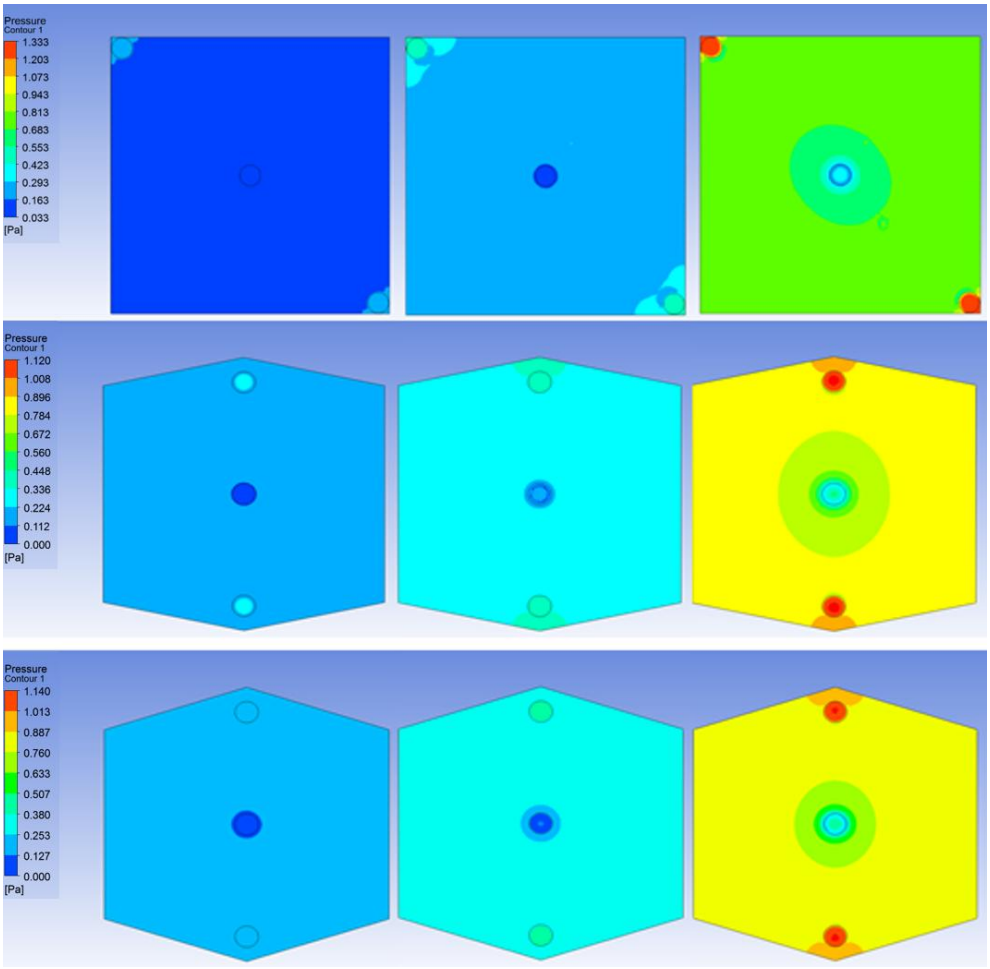

(a) 15 ml/min (b) 25 ml/min (c) 35 ml/min

Fig. 3 Analysis of the internal pressure for each cell

area. In other words, the area of the FFC cell is larger than the other cells of HFC1 and HFC2. Though it was hard to find the difference between HFC1 and HFC2, it may be considered that the pressure development in HFC1 looked slightly greater than that in HFC2.

3.1.2 Velocity vectors

Velocity vectors in each CDI cell were analyzed (Fig. 4). In FFC, dead zones were observed in two spots (indicated by circle) except the inlet edge at all the fluid rates; however, the dead zone area tends to decrease as the flow rate increases. In HFC1 and HFC2, the dead zone area was remarkably reduced at any flow rates. When HFC1 is compared with HFC2, the velocity vectors of HFC1 are more active than those of HFC2 at all flow rates. This result coincided with the previous internal pressure analysis that the internal pressure in HFC1 is slightly more developed than that in

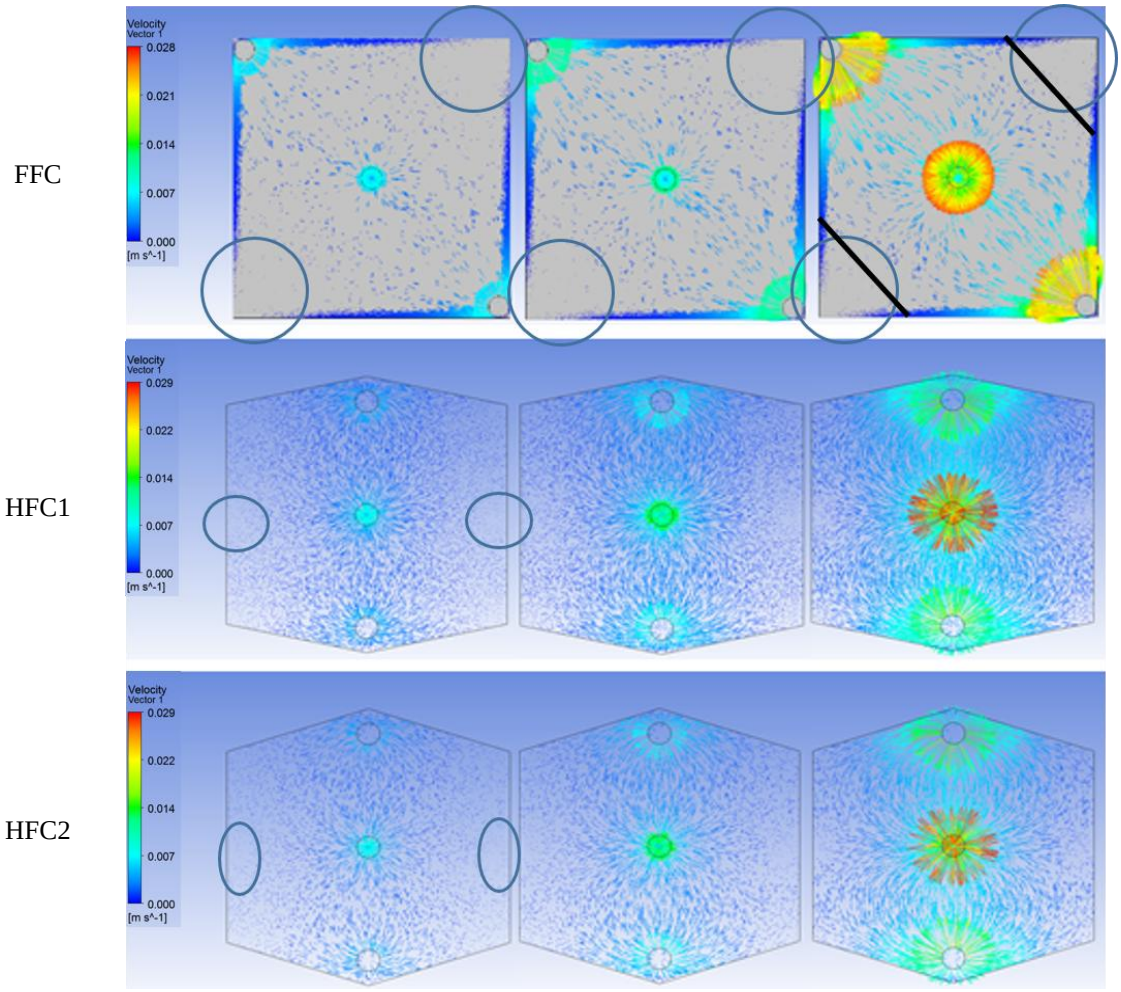

(a) 15 ml/min (b) 25 ml/min (c) 35 ml/min

Fig. 4. Velocity vectors in the flow channels of each cell

HFC2. From FFC's velocity vectors, if the dead zones indicated by circles are removed, the feed flow would cover the overall surface and the cell shape turns into the hexagon (see Fig. 4. FFC at 35 ml/min). As a result, it is regarded that the hexagon shape cell is more effective than the square cell. Also if the both lateral length in HFC1 and HFC2 is lessened, the dead zones could be perfectly removed.

3.1.3 Streamlines depending on the feed flow rate

The streamlines are depicted in Fig. 5 for all cells. Dead zones could be observed in all 3 cells. The range of the dead zone in the FFC cell is relatively wide and the second most broad is in HFC2. Finally, the HFC1 has the smallest dead zone. These results coincided in the previous studies of the internal pressure and velocity vectors.

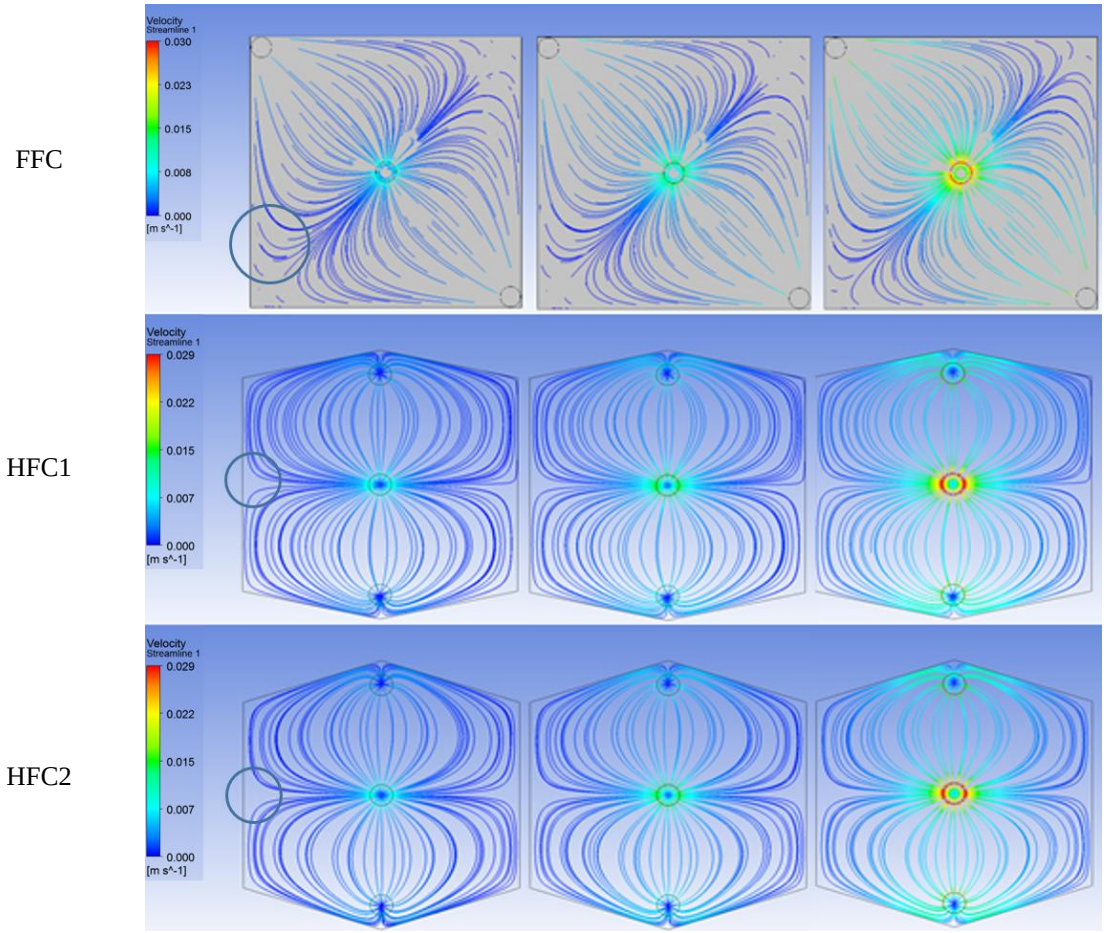

(a) 15 ml/min (b) 25 ml/min (c) 35 ml/min

Fig. 5 Streamlining vectors in the flow channels in each cell

3.2 CDI experimental analysis

To find out whether the CFD analysis matched with the experimental CDI results, a CDI experiment was carried out in terms of the effluent concentration for the existing cell (FFC) and two newly designed cells (HFC1 and HFC2). The effluent concentrations for each cell and flow rate were shown in Fig. 6. At 15 ml/min, the effluent concentrations were 145.4, 144.1, and 138.5 mg/L, respectively, for FFC, HFC1, and HFC2. Additionally, the minimum concentrations were 82, 70, and 83.5 mg/L, respectively. From these values, the salt removal efficiencies defined by Eq. 1 (Lee *et al*. 2006) were 19.4, 32.6, and 24.5% (Table 2), respectively. At 25 ml/min, the maximum effluent concentrations were 138.4, 132, and 132.9 mg/L in order, while the minimum values were 85.8, 82.6, and 88.6 mg/L. As a result, the salt removal efficiency was calculated at 16.6, 18.7, and 17.3%. Also at 35 ml/min, the maximum effluent concentrations were 139.9, 131.3, and 128.1 mg/L, and the minimum values were 86.3, 97.2, and 94 mg/L. Furthermore, the salt removal efficiencies were 16.8, 11.4, and 11.1%, respectively.

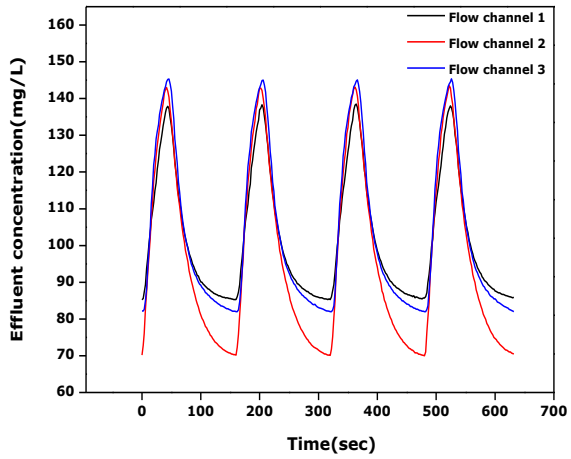

(a) 15 ml/min

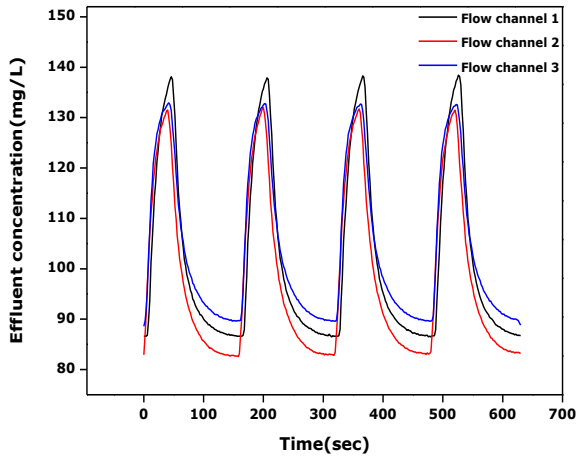

(b) 25 ml/min

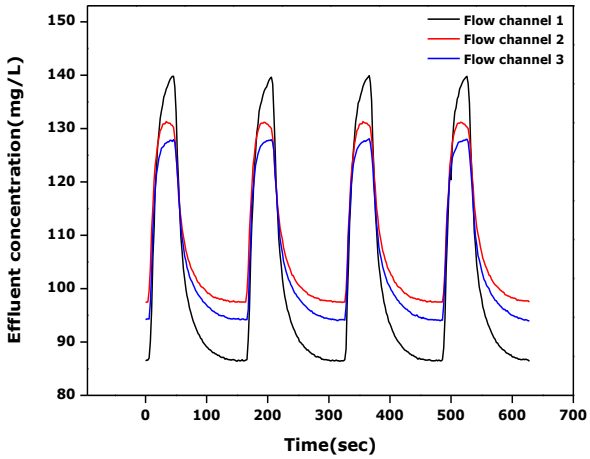

(c) 35 ml/min

Fig. 6 Effluent concentrations at (a) 15 ml/min; (b) 25 ml/min; and (c) 35 ml/min in each cell

$$\text{Salt removal efficiency (\%)} = \left(1 - \frac{C_{eff}}{C_0}\right) \times 100 \quad (1)$$

where C_{eff} is the lowest concentration of NaCl in the effluent at the adsorption step and C_0 is the concentration of feed solution.

In the previous CFD analysis, the dead zone size of the FFC cell was the largest. The maximum concentrations were the lowest while the minimum concentrations were the largest among the three cells value because the adsorption in this dead zone is limited in FFC cell. However, the maximum and minimum concentrations were shown to be erratic. In other words, there was no consistency compared between cells. The reason may be due to the different electrode areas for the 3 cell types. As mentioned, the electrode areas were 100, 75, and 70 cm^2 for FFC, HFC1 and HFC2, respectively. Therefore, we should consider the electrode area for which cell is the most effective or shows the best performance. Because the principles of the CDI process can be regarded as adsorption and desorption, the adsorption and desorption concentrations per the effective electrode area were calculated by using Eqs. (2) and (3). Eq. (2) illustrates the concentration of the adsorbed salt on the electrode surface per the electrode area whereas Eq. (3) is defined as the desorption concentration from the electrode surface per the electrode area. The calculated values are illustrated in Table 1.

$$\text{Adsorbed concentration per unit area} = \frac{(\text{Feed concentration} - \text{Minimum effluent concentration})\left(\frac{mg}{L}\right)}{\text{Effective electrode area } (cm^2)} \quad (2)$$

$$\text{Desorbed concentration per unit area} = \frac{\text{Maximum effluent concentration}\left(\frac{mg}{L}\right)}{\text{Effective electrode area } (cm^2)} \quad (3)$$

In most cases of the values calculated from Eqs. (2) and (3) at each flow rate, the efficiencies of HFC1 and HFC2 are better than that of FFC. These results coincide well with the CFD analysis. The decrease of the dead zone has a great influence on the adsorption capability at the low flow rate in particular, while at the high flow rate of 35 ml/min there is no the significant difference between the cells. This is the same as the tendency in CFD analysis in Fig. 6. Between the two cell types of HFC1 and HFC2, HFC1 is better than HFC2 at 15 ml/min, but HFC2 is better at 25 ml/min and 35 ml/min by a narrow margin. This is also a similar trend to CFD analysis. For the

Table 1 Adsorbed and desorbed concentrations by a factor of the electrode area in each cell

	15 ml/min		25 ml/min		35 ml/min	
	Adsorbed*	Desorbed**	Adsorbed*	Desorbed**	Adsorbed*	Desorbed**
FFC	0.21	1.39	0.17	1.38	0.17	1.40
HFC1	0.45	1.92	0.25	1.76	0.15	1.75
HFC2	0.30	2.08	0.27	1.90	0.17	1.83

* Calculated from Eq. (2), unit: (mg/L)/cm^2
** Calculated from Eq. (3), unit: (mg/L)/cm^2

Table 2 Salt removal efficiency by a factor of the electrode area in each cell

	Salt removal efficiency			Salt removal efficiency by a factor of electrode area		
	FFC	HFC1	HFC2	FFC	HFC1*	HFC2**
15 ml/min	19.4	32.6	24.5	19.4	43.5	35.0
25 ml/min	16.6	18.7	17.3	16.6	24.9	24.7
35 ml/min	16.8	10.4	11.1	16.8	16.1	15.9

desorbed concentration, HFC2 clearly shows the best performance than any other cell type even though the electrode area was the smallest and next is then HFC1 and FFC in order.

Next the salt removal efficiency was measured for all three types of cells at 15, 25, and 35 ml/min as shown in Table 2. However, the measured values could not be equally compared because the electrode area of each cell is different. Therefore, Eq. 4 was proposed to compare the salt removal efficiency with the consideration of the electrode area of each cell.

$$\text{Salt removal efficiency (\%)} = \left(1-\frac{C_{eff}}{C_0}\right)\left(\frac{\text{Area of electrode (HFC1 or HFC2)}}{\text{Area of standard electrode (FFC)}}\right)\times 100 \quad (4)$$

The re-calculated efficiencies on the basis of the FFC's electrode area are illustrated in Table 2. As expected, the efficiencies of HFC1 and HFC2 increased by a factor of the ratio of the electrode areas. At the low flow rate, HFC1 is more efficient than HFC2 and there is no statistical difference at a higher flow rate. In this case, the efficiencies of HFC1 and HFC2 increased 88-124% at 15 ml/min and 49-50% at 25 ml/min, respectively. No difference was observed at 35 ml/min. As the flow rate increases, the gap between FFC and HFC1 or HFC2 at each flow rate was reduced gradually and reached no difference at 35 ml/min. When the voltage is applied on the electrode, the ions in solution move to the electrode by the attraction force, which is constant, according to the applied voltage intensity. However, if the flow rate is increased gradually, the magnitude of the vector of the flow direction could be higher than the magnitude of the attraction of the electrode direction. At this point, the adsorption concentration may be reduced in any type of cell, identical to the trend in Fig. 6. Therefore, the low flow rate is better than the high flow rate in CDI operation from the viewpoint of the salt removal efficiency.

4. Conclusions

In this study, the computational fluid dynamics analysis has been conducted to investigate the flow pattern and to find the occurrence of dead zones in the existing CDI cell (FFC) and newly designed cells (HFC1 and HFC2) at 15, 25 and 35 ml/min. The separation performances between the existing and newly designed cells were compared by conducting CDI experiments in terms of the salt removal efficiency at same flow rates. From this study, several conclusions can be drawn as follows:

- In general, the internal pressure increases as the feed flow rate increases. The internal pressure of the FFC cell is lower than the new cells due to the flow channel area, where the area of the FFC cell is the largest compared to HFC1 and HFC2.
- The area of the dead zones in FFC was the largest and tended to decrease as the flow rate

increased. In HFC1 and HFC2, the dead zones were remarkably reduced at the low flow rate while at higher flow rate the dead zones were hardly comparable to the FFC.

- The decrease of the dead zone had a great influence on the adsorption capability, especially at the low flow rate in CDI experiments; however, at the high flow rate of 35 ml/min there was no significant difference between the cells. This is the same as the tendency in CFD analysis.
- The adsorbed and desorbed concentrations per electrode were greatly improved for the HFC1 and HFC2 cells at the lower flow rates.
- The salt removal efficiencies of HFC1 and HFC2 were increased 88-124% at 15 ml/min and 49-50% at 25 ml/min, respectively. There was no significant difference at 35 ml/min when compared with FFC.
- Overall, the newly designed cells of hexagon types, HFC1 and HFC2 were superior to the existing cell, FFC, from the viewpoints of the flow pattern, the adsorbed and desorbed concentrations, and the salt removal efficiency.
- Next paper will carry the CFD analysis for the regular hexagon and circle disc type cells out and experimental performance comparisons with ion exchange polymers coated onto carbon electrodes.

Acknowledgments

This research was financed by the Ministry of Education (MOE) and National Research Foundation of Korea (NRF) through the Human Resources Training Project for Regional Innovation (Grant No. 2013H1B8A2032261).

References

Biesheuvel, P.M. and van der Wal, A. (2010), "Membrane capacitive deionization", *J. Membr. Sci*., **346**(2), 256-262.

Caudle, D.D., Tucker, J.H., Cooper, J.L., Arnold, B.B. and Papastamataki, A. (1966), "Electrochemical demineralization of water with carbon electrodes", Research Report; Oklahoma University Research Institute.

Faisal, A.A., Amal, A.A.G., Irfan, S. and Nidal, H. (2014), "Application of capacitive deionization in water desalination : A review", *Desalination*, **342**, 3-15.

Fontalvo, J., Fourcade, E., Cuellar, P.C., Wijers, J.G. and Keurentjes, J.T.F. (2006), "Study of the hydrodynamics in a pervaporation module and implications for the design of multi-tubular systems", *J. Membr. Sci*., **281**(1-2), 219-227.

Ghidossi, R., Veyret, D. and Moulin, P. (2006), "Computational fluid dynamics applied to membranes: state of the art and opportunities", *Chem. Eng. Process*, **45**(6), 437-454.

Khoiruddin, K., Hakim, A.N. and Wenten, I.G. (2014), "Advances in electrodeionization technology for ionic separation- A review", *Memb. Water Treat., Int. J*., **5**(2), 87-108.

Lee, J., Park, K., Eum, H. and Lee, C. (2006), "Desalination of a thermal power plant wastewater by membrane capacitive deionization", *Desalination*, **196**(1-3), 125-134.

Lee, J.H., Bae, W.S. and Choi, J.H. (2010), "Electrode reactions and adsorption/desorption performance related to the applied potential in potential in a capacitive deionization process", *Desalination*, **258**(1-3), 159-163.

Lee, J.Y., Seo, S.J., Yun, S.H. and Moon, S.H. (2011), "Preparation of ion exchanger layered electrodes for advanced membrane capacitive deionization (MCDI)", *Water Res*., **45**(17), 5375-5380.

Li, Y.L. and Tung, K.L. (2008a), "CFD simulation of fluid flow through spacer-filled membrane module: selecting suitable cell types for periodic boundary conditions", *Desalination*, **233**(1-3), 351-358.
Li, Y.L. and Tung, K.L. (2008b), "The effect of curvature of a spacer-filled channel on fluid flow in spiral-wound membrane modules", *J. Membr. Sci.*, **319**(1-2), 286-297.
Li, H. and Zou, L. (2011), "Ion-exchange membrane capacitive deionization: A new strategy for brackish water desalination", *Desalination*, **275**(1-3), 62-66.
Lin, Z., Jin, X.H., Zhi, J.Z., Huan, L.C. and Zu, R.P. (2006), "Effect of pervaporation module structure on separation performance", *Desalination*, **193**(1-3), 166-170.
Park, N.S. (2008), "Fabrication of porous carbon electrode and its application to capacitive deionization (CDI) process", Master Dissertations; University of Gongju, Gongju, Korea. [In Korean]
Pei, X., Jorg, E.D., Dean, H. and Gary, W. (2008), "Treatment of brackish produced water using carbon aerogel-based capacitive deionization technology", *Water Res.*, **42**(10-11), 2605-2617.
Rahimi, M., Madaeni, S.S. and Abbasi, K. (2005), "CFD modeling of permeate flux in cross-flow microfiltration membrane", *J. Membr. Sci.*, **255**(1-2), 23-31.
Schwinge, J., Neal, P.R., Wiley, D.E., Fletcher, D.F. and Fane, A.G. (2004), "Spiral wound modules and spacers: Review and analysis", *J. Membr. Sci.*, **242**(1-2), 129-153.
Shirazi, M.M.A., Karkari, A., Ismail, A.F. and Matsuura, T. (2016), "Computational Fluid Dynamic (CFD) opportunities applied to the membrane distillation process: State-of-the-art and perspectives", *Desalination*, **377**, 73-90.
Takaba, H. and Nakao, S. (2005), "Computational fluid dynamics study on concentration polarization in H_2/CO separation membranes", *J. Membr. Sci.*, **249**(1-2), 83-88.
Turek, M., Mitko, K., Bandura-Zaiska, B., Ciecierska, K. and Dydo, P. (2013), "Ultra-pure water production by integrated electrodialysis-ion exchange/electrodeionization", *Memb. Water Treat., Int. J.*, **4**(4), 237-249.

CC